Electronic Supplementary Information

Rapid Chiral Analysis Based on Liquid-Phase Cyclic Chemiluminescence

Runkun Zhang, Yanhui Zhong, Zhenyu Lu, Yanlong Chen, Gongke Li*

School of Chemistry, Sun Yat-sen University, Guangzhou 510275, China

* Corresponding Authors: Gongke Li

Tel.: +86-20-84110922

Fax.: +86-20-84115107

E-mail: cesgkl@mail.sysu.edu.cn

Table of contents

1. Fabrication and working principle of liquid-phase CCL system

The CCL system mainly consists of a peristaltic pump, a high-pressure pump, a six-port injection valve with a 50 *u*L loop (V_1, C22Z-3186, Valco Instrument Co. lnc.), a microelectric six-port switching valve (V_2, C22Z-3186D, Valco Instrument Co. lnc.), a sensor cell, a time relay and a BPCL ultraweak luminescence analyzer (Institute of Biophysics, Academia Sinica, Beijing, China) equipped with a photomultiplier (PMT).

The sensor cell is composed of a quartz reactor (ED×ID×L=4×2×60 mm) and anion exchange resin with immobilized luminol (5-amino-2,3-dihydro-1,4-phthalazinedione). The immobilization procedure is according to the reported literatures.[1,2] In brief, 5 g of D201×7 anion exchange resin was immersed in NaCl solution (10%) for 20 h, then was washed with deionized water. Subsequently, anion exchange resin was washed eight times with HCI (2%) and deionized water, respectively. Activated resin was stirred with luminol (0.25 mol/L) for 12 h, then the resin was filtered, washed with deionized water and stored dry. 0.8 g of resin with immobilized luminol was packed into the quartz reactor (length × outside diameters × inside diameters = 60 mm × 6 mm ×4 mm) to fabricate sensor cell. The luminol loading was confirmed by measurement of the difference in absorbance at 360 nm from the luminol solution prior to immobilization to the luminol solution after immobilization. The amount of immobilized luminol was calculated as 2.37 mmol/g. Immobilized luminol (5-amino-2,3-dihydro-1,4-phthalazinedione) was packed into a homemade flow-through reactor to fabricate a sensor cell.

The power of V_2 in the system is controlled by the time relay to realize automatically and periodically change the direction of carrier. The peek tubing of 1/16 inch is used to connect the components of the flow path. The chiral complex samples were dissolved in a certain volume of N,N-dimethylformamide for preparation of stock solutions, and then were diluted by deionized water to prepare working solutions. A peristaltic pump was used to deliver samples at a flow rate of 10 mL/min. H_2O_2 was used as a carrier and oxidant. A high-pressure pump at a flow rate of 10 mL/min was used to deliver H_2O_2 solution.

The detection procedure is divided into three steps three stages:

(1) Sampling, the flow path is shown in Fig. S1a, the sample full fills with loop;

(2) Detection, the flow path is shown in Fig. S1b, the carrier of H_2O_2 mixes with sample and flows toward sensor cell, and H_2O_2 was catalyzed by a sample containing a metal-organic complex to produce reactive oxygen species. Subsequently, immobilized luminol in a sensor cell was oxidized by reactive oxygen species to form a 3-aminophthalate dianion in an excited state, which emitted light when returning to the ground state.[3]

(3) Circulation, the flow path alternately changes between Fig. S1b and Fig. S1c every 36 s. Thus, through automatically changing the carrier direction at the indicated period, the chemical species at different stages flowed through the sensor cell repeatedly to induce the first stage, second stage, ..., *n* th stage of CL reaction proceeds in succession.

Multistage signals that satisfy the exponential decay law were measured over time. The design of CCL sys-tem extends the observable time, and thereby the distinctions between different luminous reactions that usually are not easy to observe by conventional CL-based detection, but can be observed by CCL detection.

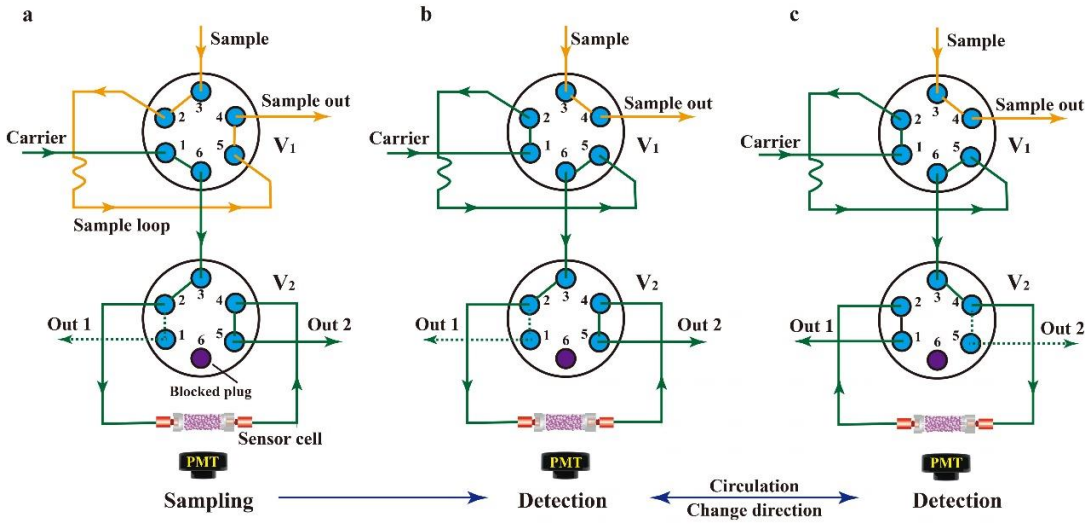

Fig. S1. The flow paths of sampling (a) and detection (b and c) in CCL system.

2. The detail information of chiral metal-organic complexes

Table S1. The detail information of chiral metal-organic complexes

Abbreviation in this paper	Chiral complex	Chemical structure	CAS
*R*1	(1*R*,2*R*)-*N*,*N*'-Bis(2-acetyl-3-oxo-2-butenylidene)-1,2-dimesitylethylenediaminato Cobalt(II)	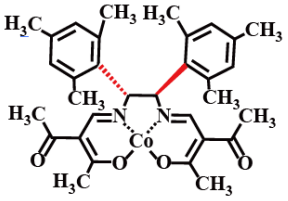	361346-80-7
*S*1	(1*S*,2*S*)-*N*,*N*'-Bis(2-acetyl-3-oxo-2-butenylidene)-1,2-dimesitylethylenediaminato Cobalt(II)	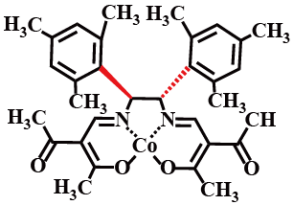	259259-80-8
*R*2	(1*R*,2*R*)-*N*,*N*'-Bis[3-oxo-2-(2,4,6-trimethylbenzoyl)butylidene]-1,2-diphenylenediaminato Cobalt(II)	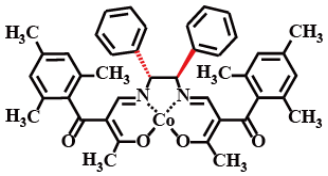	212250-92-5
*S*2	(1*S*,2*S*)-*N*,*N*'-Bis[3-oxo-2-(2,4,6-trimethylbenzoyl)butylidene]-1,2-diphenylenediaminato Cobalt(II)	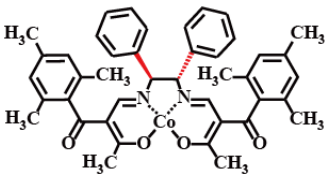	171200-71-8
*R*3	(*R*,*R*)-(-)-*N*,*N*'-Bis(3,5-di-tert-butylsalicylidene)-1,2-cyclohexanediamino cobalt(II)	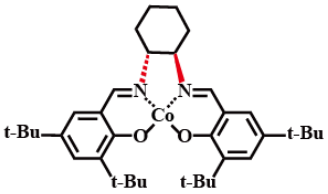	176763-62-5
*S*3	(*S*,*S*)-(+)-*N*,*N*'-Bis(3,5-di-tert-butylsalicylidene)-1,2-cyclohexanediamino cobalt(II)	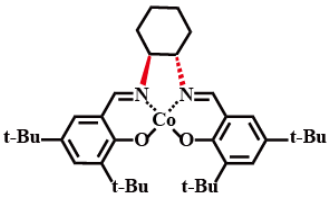	188264-84-8

3. The CCL kinetic curves of luminol-H_2O_2 system catalyzed by different chiral metal complexes

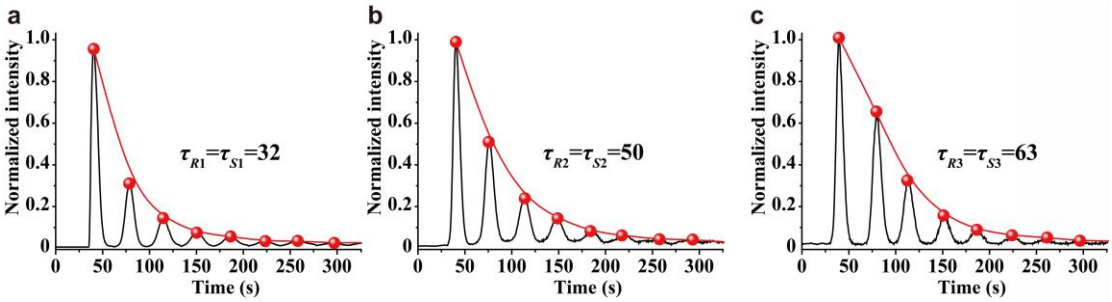

Fig. S2. The CCL kinetic curves and τ values of luminol-H_2O_2 system catalyzed by different chiral metal complexes. (a) *R*1 and *S*1, (b) *R*2 and *S*2, (c) *R*3 and *S*3.

4. The influence of H_2O_2 concentration on the CCL detection

Fig. S3 shows the influence of H_2O_2 concentration on the CCL kinetic curves of luminol-H_2O_2 system catalyzed by *S*1 with (*R*)-(+)-1-phenylethanol. It can be seen that the τ value is independent of the H_2O_2 concentration in the range of 0.02 to 0.4 mmol/L, the average τ value is 35.4 s with a relative standard deviation (RSD) of 1.6%. However, the background noise increases dramatically with the further increase in H_2O_2 concentration, and irregular CCL kinetic curve was obtained when the H_2O_2 concentration reaches 0.8 mmol/L. The low H_2O_2 concentration leads to low sensitivity, while high H_2O_2 concentration may accelerate the consumption of immobilized luminol. In view of sensitivity and lifetime of immobilized luminol, a moderate concentration of 0.05 mmol/L was selected for use.

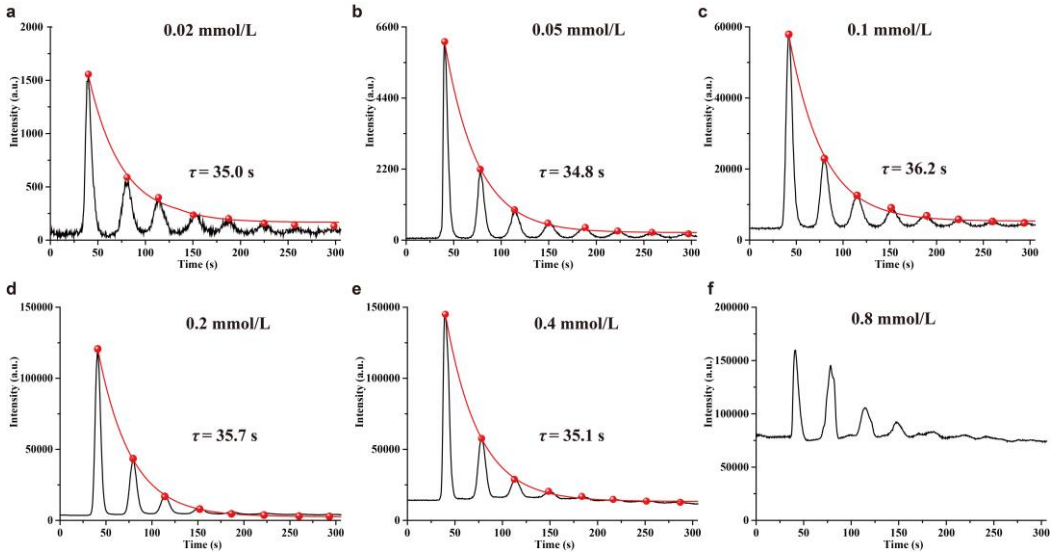

Fig. S3. The influence of H_2O_2 concentration on the CCL kinetic curves. The concentrations of both *S*1 and (*R*)-(+)-1-phenylethanol are 0.1 mmol/L.

5. The reproducibility of CCL detection

The reproducibility of immobilized luminol within the same batch and between different batches were investigated by using *S*1 to measure (*R*)-(+)-1-phenylethanol. Fig. S4 shows that CCL kinetic curves obtained by the first, fifteenth, twenty-fifth and twenty-sixth tests. It can be seen that the background noise increases (I_0) and the luminescence intensity (A) decreases gradually with increasing test number, but the lifetime (τ) of the multistage signals on CCL kinetic curve almost remain stable within 25 replicates. Irregular CCL kinetic curve was observed as further increase in test number (Fig. S4d). The RSD of τ values measured by 25 replicate determinations is 3.7% (Fig. S5a), and the RSD of τ values measured by 5 different batches of immobilized luminol is 4.2% (Fig. S5b). The above results indicate that the consumption of immobilized luminol may also cause the decline of the CL intensity, but one reactor packed with fresh immobilized luminol allows about 25 times effective CCL detection. In addition, the stable τ values among different batches of immobilized luminol allows us to repack fresh immobilized luminol for the next assays if the previous immobilized luminol has lose its performance.

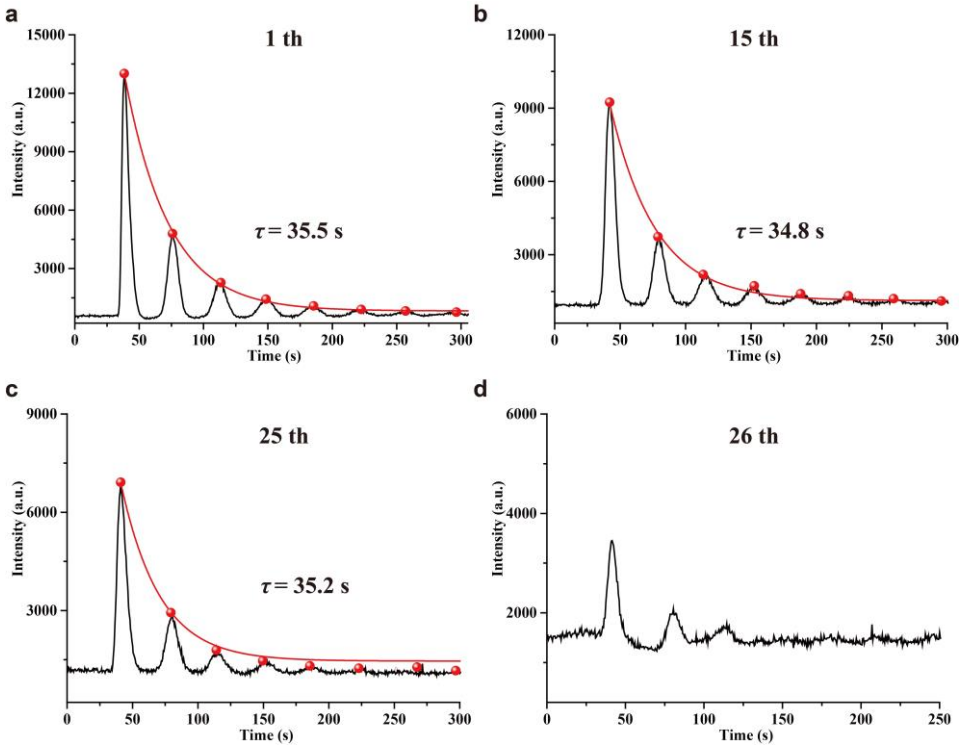

Fig. S4. The CCL kinetic curves and τ values obtained by the first (a), fifteenth (b), twenty-fifth (c) and twenty-sixth (d) tests. The concentrations of *S*1 and (*R*)-(+)-1-phenylethanol are 0.1 mmol/L, the concentration of H_2O_2 is 0.05 mmol/L.

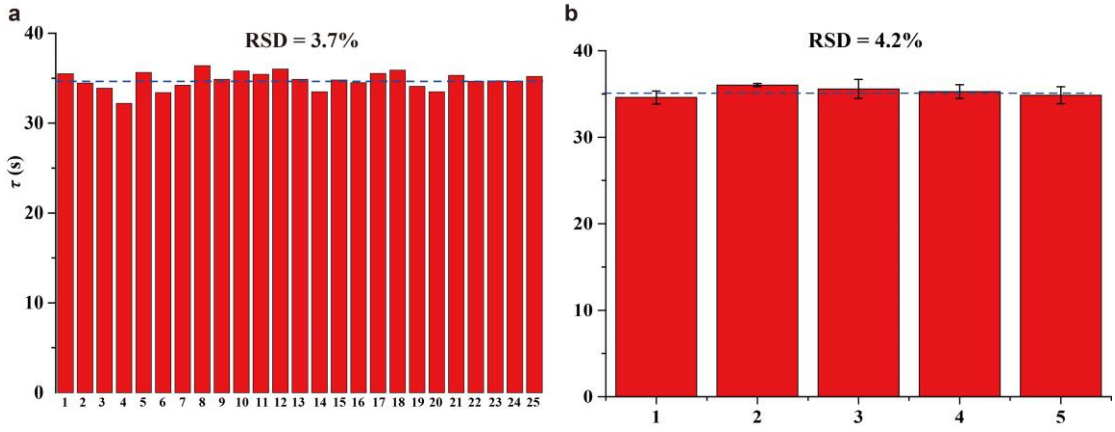

Fig. S5. The reproducibility of immobilized luminol within the same batch (a) and between different batches (b). The concentrations of *S*1 and (*R*)-(+)-1-phenylethanol are 0.1 mmol/L, the concentration of H_2O_2 is 0.05 mmol/L.

6. τ values of 6 chiral hosts to 12 guests at different concentrations

Table S2. τ values of 6 chiral hosts to 12 guests at different concentrations[a]

Chiral guest	Concentration (mmol/L)	Chiral host					
		*R*1	*S*1	*R*2	*S*2	*R*3	*S*3
A	0.005	64.9	35.2	37.4	46.6	24.2	32.9
	0.05	64.0	35.3	37.9	47.6	24.9	33.0
	0.1	65.0	35.1	37.8	46.2	24.6	33.3
B	0.005	38.5	51.5	63.6	40.0	42.7	47.7
	0.05	39.1	52.3	63.5	40.5	43.4	47.4
	0.1	39.4	51.0	63.0	40.8	43.2	47.9
C	0.005	53.3	71.4	30.3	45.0	55.4	33.9
	0.05	52.1	70.5	30.4	45.6	54.0	33.1
	0.1	52.9	70.2	30.7	45.6	55.1	33.4
D	0.005	38.6	50.0	25.1	40.3	20.0	27.6
	0.05	37.2	50.7	25.5	40.0	20.1	27.9
	0.1	38.9	50.6	25.0	41.1	19.2	27.6
E	0.005	57.8	38.9	20.6	56.5	44.1	53.2
	0.05	59.8	39.6	23.9	56.3	44.9	53.8
	0.1	57.3	38.6	20.4	56.6	43.5	53.5
F	0.005	46.5	53.3	28.1	34.2	28.3	34.7
	0.05	46.7	53.0	28.1	35.4	29.7	36.0
	0.1	46.4	53.9	28.0	34.6	28.7	34.3
G	0.005	12.1	108.0	60.5	26.3	13.1	51.8
	0.05	11.9	108.0	60.8	26.6	13.2	51.3
	0.1	12.4	106.9	60.3	26.3	13.7	51.5
H	0.005	21.5	22.3	26.3	82.0	52.5	29.2
	0.05	20.4	21.1	27.8	82.6	52.2	29.5
	0.1	20.4	21.9	26.5	82.2	52.3	29.4
I	0.005	50.2	37.2	18.8	30.0	45.8	102.9
	0.05	49.2	37.5	17.5	30.0	45.4	108.0
	0.1	49.5	37.5	18.1	29.3	45.7	103.8
J	0.005	72.8	23.3	82.3	47.3	80.1	73.6
	0.05	72.9	23.0	82.1	48.9	80.4	73.0
	0.1	76.1	23.8	81.0	48.7	80.6	72.6
K	0.005	31.2	14.4	17.5	60.0	31.4	84.4
	0.05	31.9	14.7	18.8	60.0	31.1	86.6
	0.1	31.6	14.7	18.5	59.1	32.4	84.4
L	0.005	23.4	32.0	36.9	55.7	41.6	66.6
	0.05	24.1	32.6	37.4	55.5	41.1	67.3
	0.1	23.5	32.4	37.1	55.5	41.5	66.2

[a]A: (*R*)-(+)-1-phenylethanol; B: (*S*)-(-)-1-phenylethanol; C: (*R*)-(-)-2-pentanol ; D: (*S*)-(+)-2-pentanol; E: (*R*)-(-)-2-phenylglycinol; F: (*S*)-(+)-2-phenylglycinol; G: (*R*)-3-amino-3-phenylpropan-1-ol; H: (*S*)-3-amino-3-phenylpropan-1-ol; I: *D*-(-)-tartaric acid; J: *L*-(+)-tartaric acid; K: *D*-(-)-mandelic acid; L: *L*-(+)-mandelic acid.

7. ^{1}H NMR spectra of *R*1 and *S*1 before and after the addition of 1-phenylethanol enantiomers

The ^{1}H NMR spectra of *R*1 and *S*1 with equimolar amounts of (*R*)-(+)-1-phenylethanol and (*S*)-(-)-1-phenylethanol were performed in DMSO-d6 using a 600-MHz NMR spectrometer under -80 ℃. As shown in Fig. S6, broader NMR peaks of *R*1 and *S*1 were obtained as a result of the high-spin cobalt ions being weakly antiferromagnetic, which interferes with the magnetic environment around the ligand. Additions of 1-phenylethanol enantiomers result in peak disappearance at δ=2.16 ppm and δ=1.89 ppm of *R*1 and *S*1. Additions of 1-phenylethanol into *S*1 can eliminate the interference of cobalt ions on the magnetic environment around the ligand, but *R*1 still exhibits antiferromagnetism. However, ^{1}H NMR spectra in Fig. S3 clearly show that NMR spectroscopy cannot effectively resolve the enantiomers of 1-phenylethanol when using *R*1 or *S*1 as host.

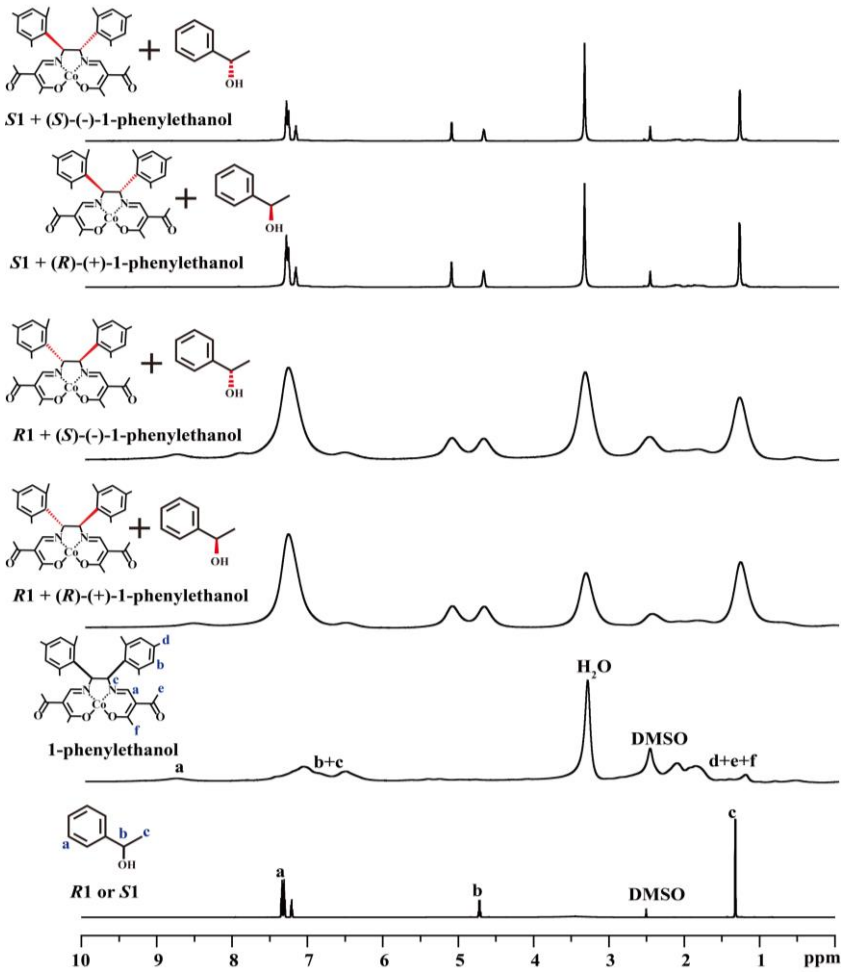

Fig. S6. ^{1}H NMR spectra of *R*1 and *S*1 before and after the addition of 1-phenylethanol enantiomers.

8. Experiment of static injection chemiluminescence

Static injection is one of the important approaches for chemiluminescence (CL) measurement, it allows measurement of the full intensity time curve. In order to compare the kinetic curves obtained by CCL and static injection, static injection CL measurement was performance. 1 mL of luminol (0.1 mmol/L) solution and H_2O_2 solution (0.05 mmol/L) were added into an cuvette, and then 50 μl of *R*1, *S*1, *R*1+(*R*)-(+)-1-phenylethanol (*R*1+*R*) , *R*1+(*S*)-(-)-1-phenylethanol (*R*1+*S*) and *S*1+ (*R*)-(+)-1-phenylethanol (*S*1+*R*) and *S*1+ (*S*)-(-)-1-phenylethanol (*S*1+*S*) at different concentrations (0.01, 0.05 and 0.1 mmol/L) were injected to initiate the CL emission, respectively. Three parallel measurements were performed. The CL kinetic curves showing CL intensity as a function of time after injection were monitored by the detector. The intensity decay curves were fitted with first-order exponential function to obtain τ value of each kinetic assay, the results are shown in Fig. S7.

It seems that there exist subtle differences among the CL kinetic curves of different reaction system obtained by static injection. However, the decay speed of the CL intensity is very quick, rending short lifetimes (small τ values) were observed. The τ values of different kinetic curve are in the range from 1.0 to 3.6 s, the narrow τ-range means low resolution. In addition, a subtle fluctuation in the small τ value will result in a large RSD. For example, the τ values of *R*1+(*R*)-(+)-1-phenylethanol, *R*1+(*S*)-(-)-1-phenylethanol systems at 0.1 mmol/L are 3.1 ± 0.5 and 2.2 ± 0.5, respectively. The corresponding RSDs are 16.1% and 22.7%. It is difficult to discriminate chiral compounds according to the τ values of CL kinetic curves obtained by static injection.

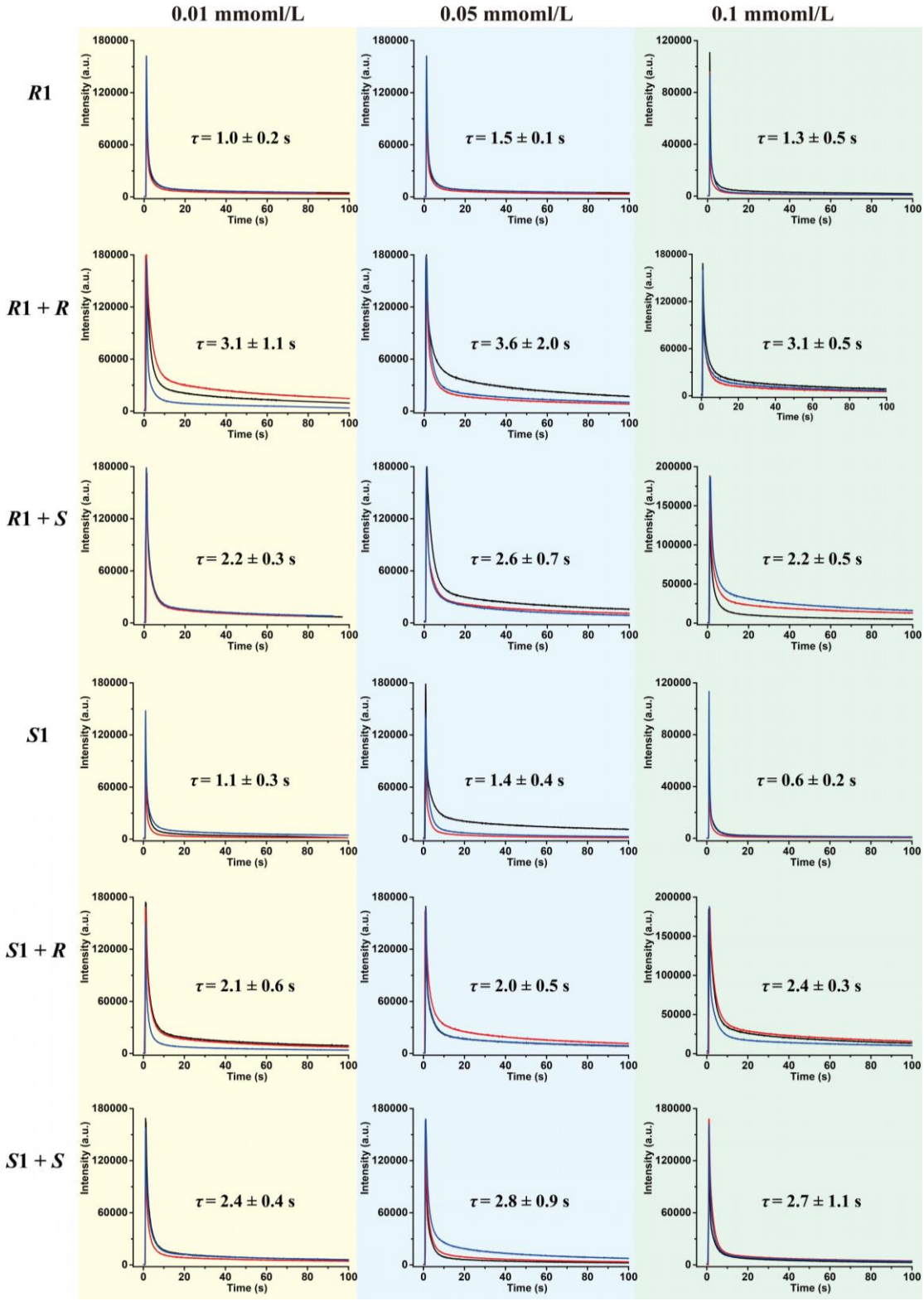

Fig. S7. The CL kinetic curves and corresponding τ values of different chiral host-guest systems obtained by static injection. The concentrations of luminol and H_2O_2 are 0.1 mmol/L and 0.05 mmol/L, respectively. The blue, red and black lines in each inset stand for the CL kinetic curves of three replicates. *R* and *S* stand for (*R*)-(+)-1-phenylethanol and (*S*)-(-)-1-phenylethanol, respectively.

9. Determination of *ee* values of 1-phenylethanol by using complex *R*1 and *S*1

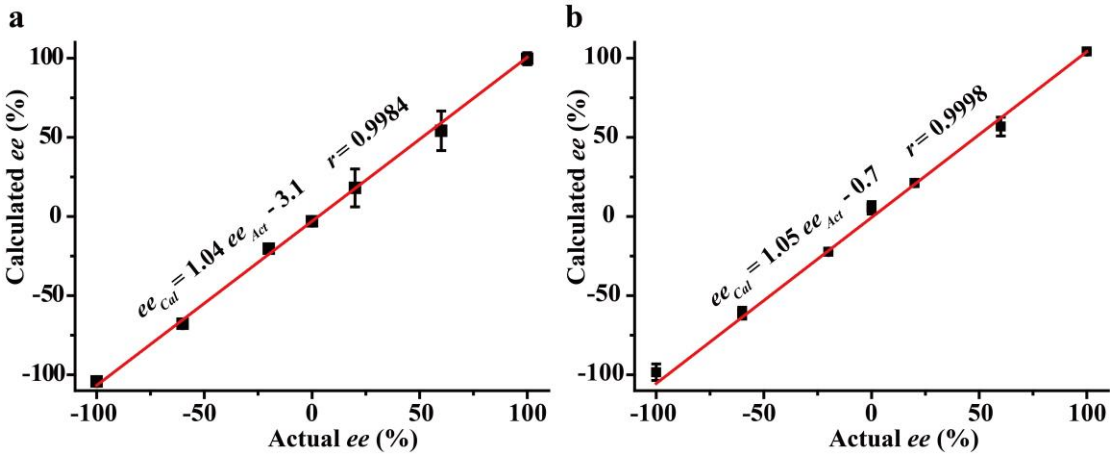

Fig. S8. Linear relationship between calculated *ee* values and actual *ee* values using *R*1 (a) and *S*1 (b) as hosts, *n*=3.

Table S3. Quantitative determination of *ee* values of 1-phenylethanol by using complex *R*1 and *S*1

*R*1 as host			*S*1 as host		
Actual *ee* (%)	Calculated *ee* (%)	Absolute error (%)	Actual *ee* (%)	Calculated *ee* (%)	Absolute error (%)
-100.0	-104.2	-4.2	-100.0	-98.4	1.6
-60.0	-66.9	-6.9	-60.0	-61.1	-1.1
-20.0	-21.5	-1.5	-20.0	-22.3	-2.3
0.0	-1.5	-1.5	0.0	-2.8	-2.8
20.0	18.1	-1.9	20.0	21.1	1.1
60.0	64.6	4.6	60.0	56.8	-3.2
100.0	99.6	-0.4	100.0	104.2	4.2

10. Experiments for monitoring of Walden inversion reaction of (*S*)-(-)-1-phenylethanol

Table S4. Instrument operating parameters of HPLC for monitoring of Walden inversion reaction of (*S*)-(-)-1-phenylethanol

Items	Parameters
Column	Chiral INB 5u, 250*4.6 mm, supplied by Guangzhou FIM Scientific Instrument Co., Ltd
Carrier	*n*-Hexane : *iso*-Propanol =96:4
Flow rate	0.7 mL/min
Detector	UV
Wavelength	210 nm

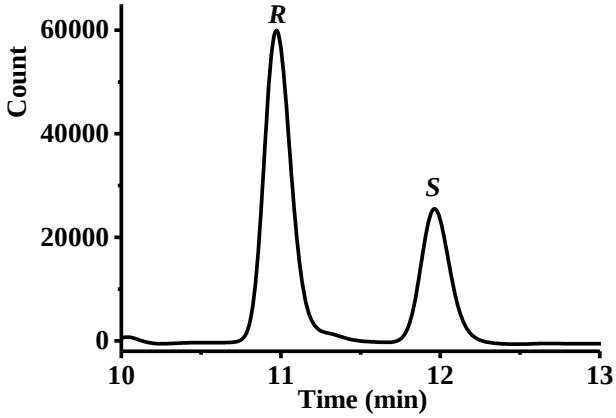

Fig. S9. Standard chromatogram of (*R*)-(+)-1-phenylethanol (10.9 min) and (*S*)-(-)-1-phenylethanol (11.8 min).

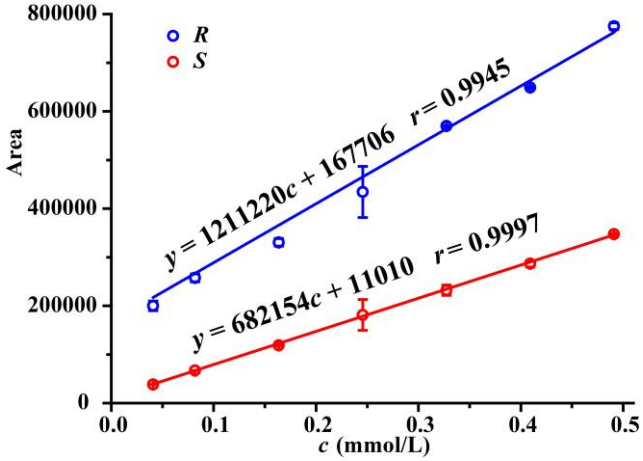

Fig. S10. Calibration curves of (*R*)-(+)-1-phenylethanol and (*S*)-(-)-1-phenylethanol measured by HPLC.

Table S5. The *ee* values versus time monitored by the CCL and HPLC

	55 °C					65 °C				
Reaction time (min)	*ee*(%)$_{CCL}$	SD	*ee* (%)$_{HPLC}$	SD	Absolute error (%)	*ee* (%)$_{CCL}$	SD	*ee* (%)$_{HPLC}$	SD	Absolute error (%)
5	-53.4	7.4	-54.3	1.6	0.9	-62.8	6.9	-68.4	4.8	5.6
10	-41.8	8.0	-35.8	0.3	-6.0	-24.2	3.2	-31.2	3.4	7.0
20	-28.3	1.6	-27.1	5.5	-1.2	-12.9	3.2	-10.4	4.3	-2.5
40	0.6	1.1	4.8	8.8	-4.2	50.9	3.1	47.7	3.8	3.2
60	4.5	2.7	7.9	7.7	-3.4	70.8	2.7	68.7	0.8	2.1
80	54.1	4.1	61.2	7.6	-7.1	93.4	8.2	91.5	0.4	1.9
120	90.0	1.1	94.5	3.6	-4.5	106.5	3.7	111.8	0.4	-5.3
160	92.2	8.5	87.9	0.7	4.3	113.6	2.7	108.4	0.9	5.2
200	96.0	10.6	96.1	2.1	-0.1	111.0	6.4	112.1	0.3	-1.1
240	110.1	6.2	106.5	11.9	3.6	107.5	1.4	108.1	2.2	-0.6

11. Experiments for detection of ibuprofen samples

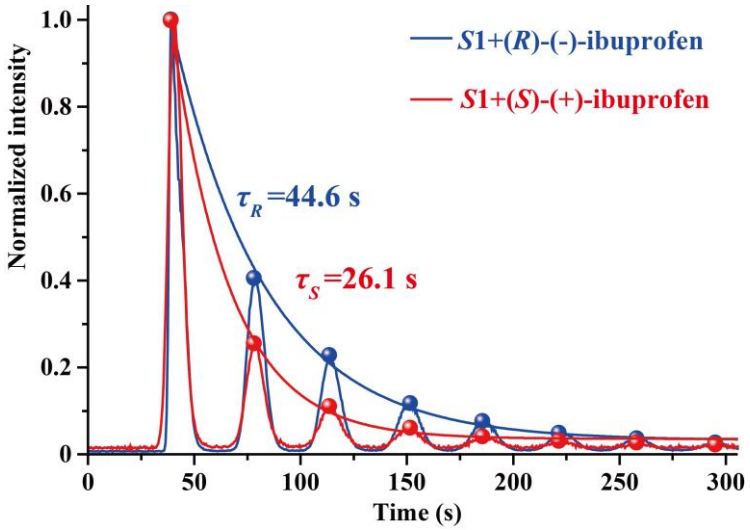

Fig. S11. The CCL kinetic curves of luminol-H_2O_2 system catalyzed by *S*1 with ibuprofen.

Table S6. Instrument operating parameters of HPLC for detection of ibuprofen

Items	Parameters
Column	Chiral MJ(2)-RH 5u, 250*4.6 mm, supplied by Guangzhou FIM Scientific Instrument Co., Ltd
Carrier	MeOH: HCOOH=90:10
Flow rate	0.8 mL/min
Detector	UV
Wavelength	220 nm

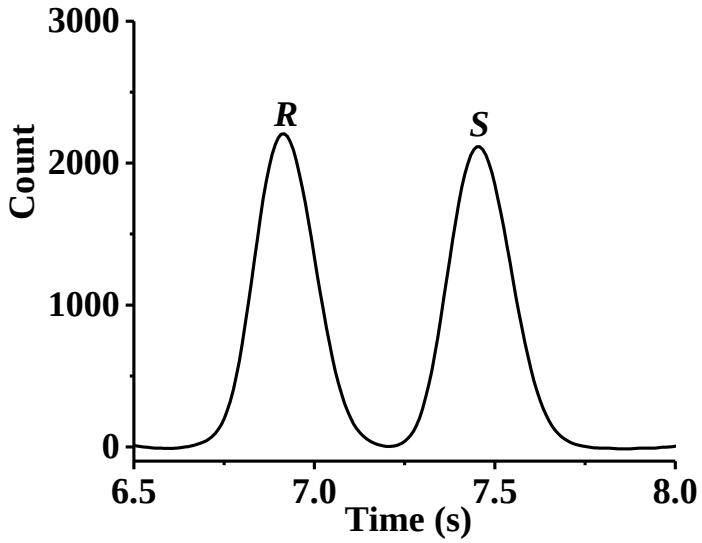

Fig. S12. Standard chromatogram of (*R*)-(-)-ibuprofen (6.9 min) and (*S*)-(+)-ibuprofen (7.4 min).

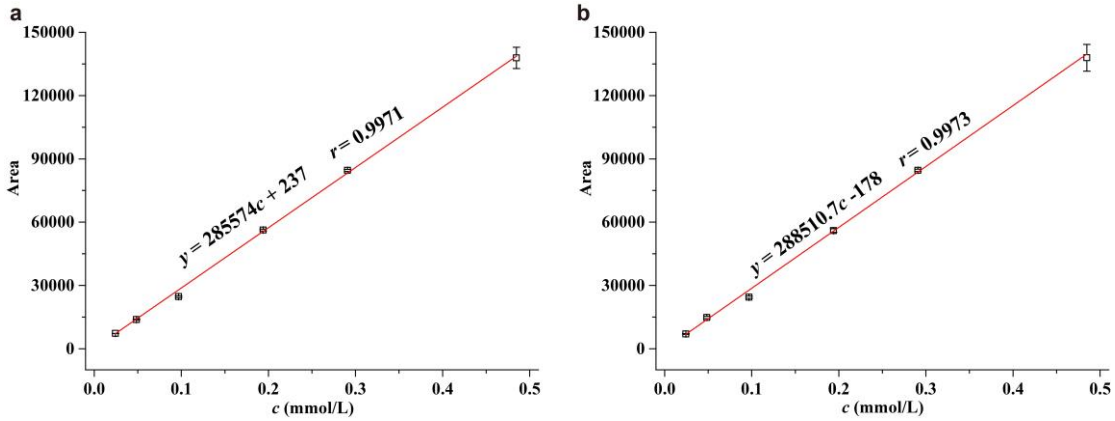

Fig. S13. Calibration curves of (*R*)-(-)-ibuprofen (a) and (*S*)-(+)-ibuprofen (b) measured by HPLC.

12. Raman spectra of the new adducts

The Raman spectra of four adducts were recorded using Renishaw, InVia Qontor spectrometer (785 nm laser excitation; laser power, 335 mW*50%; exposure time 10 s) The results are shown in Fig. S14.

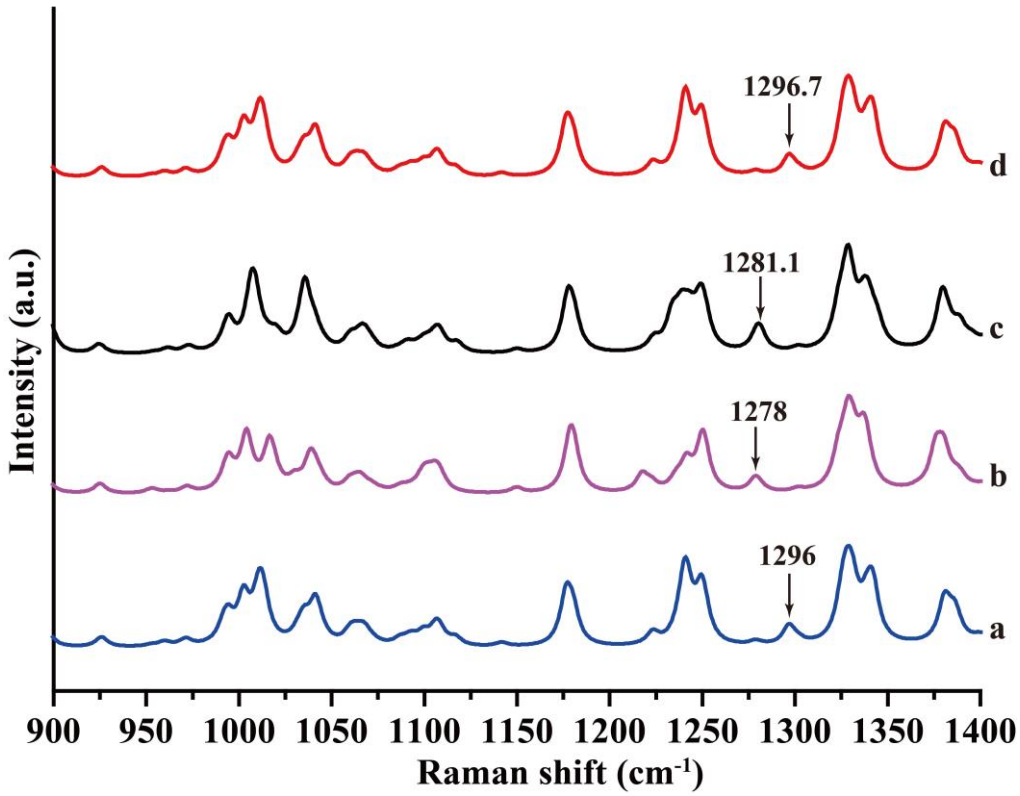

Fig. S14. The Raman spectra of four adducts. a: *R*1+*R*; b: *R*1+*S*; c: *S*1+*R*; d: *S*1+*S*.

13. **The reaction kinetics of different chrial substances-catalyzed luminol-H_2O_2 reactions**

The reaction kinetics of luminol-H_2O_2 reactions catalyzed by different chrial substances (*R*1, *R*1+*R*, *R*1+*S*, *S*1, *S*1+*R* and *S*1+*S*) were investigated by using HPLC to monitor the consumption rate of luminol. The luminol (0.1 mmol/L), H_2O_2 (0.05 mmol/L) and chiral compounds (0.1 mmol/L) were added into a cuvette, the change trends of luminol area versus time were monitored at 384 nm. The results are shown in Fig. S15.

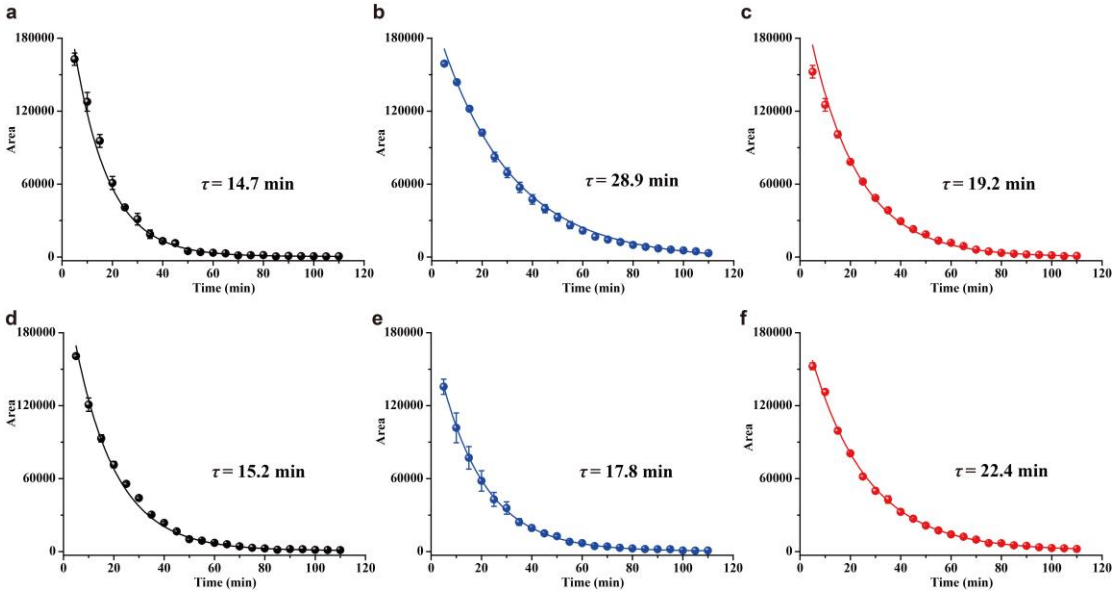

Fig. S15. The change trends of luminol area versus time. a: *R*1; b: *R*1+*R*; c: *R*1+*S*; d: *S*1; e: *S*1+*R*; f: *S*1+*S*. Carrier: MeOH: H_2O=40:60; flow: 1.2 mL/min.

14. Reference

1. B. X. Li, Z. J. Zhang and Y. Jin, *Sens. Actuators, B* 2001, **72**, 115-119.
2. T. Okamoto, K. Tanaka, H. Goto, J. M. Lin, M. Yamada and Y. Asano, *Anal. Commun.* 1999, **36**, 181-183.
3. L. Rose and T. D. Waite, *Anal. Chem.* 2001, 73, 5909−5920.